Absolute differential positronium-formation cross-sections

M. Shipman, S. Armitage, J. Beale[a], S. J. Brawley, S. E. Fayer,
A. J. Garner, D. E. Leslie[b], P. Van Reeth and G. Laricchia
UCL Department of Physics and Astronomy, University College London, Gower Street, London, WC1E 6BT
[a] *now at Atomic Weapons Establishment, Aldermaston, Reading, RG7 4PR, UK*
[b] *now at Brunel University London, Kingston Lane, Uxbridge, UB8 3PH, UK*

The first absolute experimental determinations of the differential cross-sections for the formation of ground-state positronium are presented for He, Ar, H_2 and CO_2 near 0°. Results are compared with available theories. The ratio of the differential and integrated cross-sections for the targets exposes the higher propensity for forward-emission of positronium formed from He and H_2.

PACS numbers: 36.10.Dr, 34.80.Bm, 34.80.Uv

The formation of positronium (Ps, the bound state of an electron and a positron) is an important channel in the scattering of positrons from atoms and molecules e.g. [1–3], accounting for up to 50% of the total cross-section, with experimental and theoretical investigations of its integrated formation cross-sections available for a wide range of atoms and simple molecules, e.g. [3–5]. Recent experimental studies also include its formation in an excited state [6] or accompanied by ionic excitation [7]. However, whilst theoretical predictions for the differential Ps formation cross-section ($\frac{\mathrm{d}Q_{\mathrm{Ps}}}{\mathrm{d}\Omega}$) are available for atomic [8–16] and molecular [17, 18] hydrogen, the noble gases [9, 16, 19–29] and the alkali metals [30–34], experimental data remain scarce. Indeed, available measurements are confined to H_2 [35], Ar and Kr [36, 37] and, due to unknown positron and Ps detection efficiencies ($\varepsilon_{\mathrm{d}}^{+}$ and $\varepsilon_{\mathrm{d}}^{\mathrm{Ps}}$, respectively), these results are *relative* and susceptible to *energy-dependent* systematic errors.

In this communication, we present the first absolute experimental determinations of $\frac{\mathrm{d}Q_{\mathrm{Ps}}}{\mathrm{d}\Omega}$ for He, Ar, H_2 and CO_2. The values are extracted from measurements of the production efficiency of the Ps beam at UCL and thus correspond to a small angle around 0°. An absolute scale has been assigned by using experimental values for the ratio $R_{\mathrm{d}} = \varepsilon_{\mathrm{d}}^{+}/\varepsilon_{\mathrm{d}}^{\mathrm{Ps}}$ [38, 39], together with a recent finding that, although $\varepsilon_{\mathrm{d}}^{+}$ and $\varepsilon_{\mathrm{d}}^{\mathrm{Ps}}$ may individually vary significantly (e.g. due to different detector-types, ages, and settings), R_{d} does not do so appreciably [40]. Where possible, the results are compared with theoretical determinations at zero degrees.

Details of the experimental arrangement employed at UCL for producing a beam of Ps atoms, together with a review of recent advances, may be found in [41]. In brief, the Ps beam is produced by charge-exchange of positrons (e^+) with a target gas (A), i.e. $e^+ + A \longrightarrow Ps + A^+$, and detected downstream by a channel-electron-multiplier (CEM or CEMA) in coincidence with one or more γ-ray detectors (e.g. CsI or NaI). The beam has been found to be composed predominantly of ground-state atoms [42, 43].

Depending on the relative spin orientation of its constituents, ground-state Ps may be formed in an ortho- ($^3S_1$) or para- ($^1S_0$) state. The two are characterized by lifetimes differing by three orders of magnitude (142 ns and 125 ps, respectively) and different annihilation modes (dominantly 3-γ and 2-γ, respectively). Only ortho-Ps reaches the detection region.

In order to determine $\frac{\mathrm{d}Q_{\mathrm{Ps}}}{\mathrm{d}\Omega}$(a measure of the probability that Ps is emitted within a solid angle $d\Omega = 2\pi sin\theta d\theta$), we have measured the number of Ps atoms ($\varepsilon_{\mathrm{d}}^{\mathrm{Ps}} N_{\Delta\Omega}^{\mathrm{Ps}}$) detected in a small solid angle ($\Delta\Omega$) per measured incident positrons ($\varepsilon_{\mathrm{d}}^{+} N_{+}$). These here define the measured Ps beam production efficiency ($\epsilon_{\mathrm{Ps}}^{\mathrm{m}}$) according to

$$\epsilon_{\mathrm{Ps}}^{\mathrm{m}} = \frac{\varepsilon_{\mathrm{d}}^{\mathrm{Ps}} N_{\Delta\Omega}^{\mathrm{Ps}}}{\varepsilon_{\mathrm{d}}^{+} N_{+}} = \frac{\epsilon_{\mathrm{Ps}}}{R_{\mathrm{d}}} \mathrm{e}^{-t/\tau_{\mathrm{Ps}}}, \qquad (1)$$

where τ_{Ps} is the lifetime of ortho-Ps, t its flight-time to the detector and ϵ_{Ps} the 'true' Ps beam production efficiency. In Eq.(1), $\epsilon_{\mathrm{Ps}}^{\mathrm{m}}$ may be seen to depend on the (energy-dependent) ratio of the positron to positronium detection efficiencies R_{d} also determined by our group [38–40].

By studying the variation of ϵ_{Ps} with gas pressure, optimum beam operating conditions may be determined for a given target and Ps energy [39, 40, 44, 45]. An example is shown in Figure 1 for production of 20 eV Ps from CO_2. Here ϵ_{Ps} may be seen to increase and then decrease with increasing pressure. This variation may be expressed as:

$$\epsilon_{\rm Ps} = (1 - \exp(-\rho L_+ Q_{\rm T}^+)) \left(\frac{2\pi}{Q_{\rm T}^+} \int_0^{\theta'} \frac{{\rm d}Q_{\rm Ps}}{{\rm d}\Omega} \sin\theta \, {\rm d}\theta \right) \exp\left(-\rho L_{\rm Ps} Q_{\rm T}^{\rm Ps}\right), \quad (2)$$

where the first term in brackets corresponds to the total fraction of positrons scattered in a gas region of number density ρ and length L_+, the second to the probability that Ps will be formed within a small pencil angle θ' and the third term to the transmission probability of Ps through the gas region of length $L_{\rm Ps}$, $Q_{\rm T}^+$ and $Q_{\rm T}^{\rm Ps}$ being the positron-gas and Ps-gas total cross-sections, respectively. If the differential cross-section does not vary too rapidly over the small range $0 \leq \theta \leq \theta'$ — namely (1.1-1.7)° in this work — the second term may be approximated as:

$$\frac{2\pi}{Q_{\rm T}^+} \int_0^{\theta'} \frac{{\rm d}Q_{\rm Ps}}{{\rm d}\Omega} \sin\theta \, {\rm d}\theta \simeq \left\langle \frac{{\rm d}Q_{\rm Ps}}{{\rm d}\Omega} \right\rangle \frac{\Delta\Omega}{Q_{\rm T}^+}, \quad (3)$$

where $\Delta\Omega$ is the (small) detection solid angle and $\langle \frac{{\rm d}Q_{\rm Ps}}{{\rm d}\Omega} \rangle$ is the average value of $\frac{{\rm d}Q_{\rm Ps}}{{\rm d}\Omega}$ over the range (0 - θ'). Explicitly allowing for the fact that Ps may be formed anywhere along the gas cell of effective length L, we may express $L_{\rm Ps} = L - \ell_+$, where ℓ_+ is the variable of integration in the following equation:

$$\epsilon_{\rm Ps}^{\rm m} \simeq \frac{3}{4} \frac{1}{R_{\rm d}} \frac{1}{Q_{\rm T}^+} \left\langle \frac{{\rm d}Q_{\rm Ps}}{{\rm d}\Omega} \right\rangle \int_0^L \Big[\exp(-\rho \ell_+ Q_{\rm T}^+) \times \exp\left(-\rho (L - \ell_+) Q_{\rm T}^{\rm Ps}\right) \left(\frac{\pi r^2}{(L - \ell_+ + d)^2} \right) \times \exp\left(-\frac{(L - \ell_+ + d)}{\tau_{\rm Ps}} \sqrt{\frac{m}{E_{\rm Ps}}} \right) \Big] \rho Q_{\rm T}^+ \, {\rm d}\ell_+, \quad (4)$$

which allows for Ps formation and scattering along L, as well as for the corresponding variations in detection solid angle and in-flight Ps annihilation. Specifically, the factor of 3/4 arises from the spin multiplicity of Ps; the third and fourth terms in the integral represent, respectively, the detection solid angle and in-flight survival probability: $L - \ell_+ + d$ being the Ps flight path to the detector of effective area πr^2, $E_{\rm Ps}$ is the Ps kinetic energy and m the mass of the positron.

Approximating the integral in Equation 4 with a summation over ℓ_+ in steps $\Delta\ell_+$ such that $\rho \Delta\ell_+ Q_{\rm T}^+ \to 0$, and re-arranging, we obtain for the absolute differential Ps formation cross-section:

$$\frac{{\rm d}Q_{\rm Ps}}{{\rm d}\Omega} \simeq \left\langle \frac{{\rm d}Q_{\rm Ps}}{{\rm d}\Omega} \right\rangle \simeq \frac{4}{3} \frac{\epsilon_{\rm Ps}^{\rm m} R_{\rm d}}{\rho \Delta \ell_+} \times \left\{ \sum_{\ell_+=0}^{L} \left[\exp(-\rho \ell_+ Q_{\rm T}^+) \exp\left(-\rho (L - \ell_+) Q_{\rm T}^{\rm Ps}\right) \times \left(\frac{\pi r^2}{(L - \ell_+ + d)^2} \right) \times \exp\left(-\frac{(L - \ell_+ + d)}{\tau_{\rm Ps}} \sqrt{\frac{m}{E_{\rm Ps}}} \right) \right] \right\}^{-1}, \quad (5)$$

where the approximation $\frac{{\rm d}Q_{\rm Ps}}{{\rm d}\Omega} \simeq \langle \frac{{\rm d}Q_{\rm Ps}}{{\rm d}\Omega} \rangle$ has been made given the small acceptance angle used in this work. The values for the positron and Ps total cross-sections have been taken from available literature, specifically from [46–49] and [50–52] respectively, interpolating when necessary. At 120 eV for He and Ar, where Ps data were not available, the cross-sections were estimated by extrapolation, guided by the findings of Brawley et al. [50] on the similarity with equivelocity-electron results. The effective length of the gas cell (L) has been determined by measuring positron beam attenuations and normalising to known cross-section values across a number of targets [46–48, 53–57].

Figure 2 displays the $\frac{{\rm d}Q_{\rm Ps}}{{\rm d}\Omega}$ values obtained from $\epsilon_{\rm Ps}$ (shown in Figure 1) and Equation 5. As expected, in Figure 2, the cross-section is seen to be (within errors) independent of pressure. However, in some cases where this was not found to be so, $Q_{\rm T}^+$ and/or $Q_{\rm T}^{\rm Ps}$ were varied in order to achieve pressure-independence and to estimate the associated uncertainty on $\frac{{\rm d}Q_{\rm Ps}}{{\rm d}\Omega}$ ($\leq 10\%$ in all cases, except for CO_2 at 139 eV where $\leq 18\%$ applies). An additional systematic uncertainty arises from that in R_d, estimated to be +8% and -(20-30)% [38]. At each energy, the absolute differential Ps formation cross-section has been computed as the weighted mean of the results across the pressure range if within errors, else the mean and standard error are reported. As a check of self-consistency, the variation of $\epsilon_{\rm Ps}$ predicted by this weighted mean is also shown in Figure 1.

In Figure 3, absolute differential Ps formation cross-sections in positron collisions with He and Ar are presented and compared with available theories at zero degrees. For both targets, the experimental data increase with increasing energy to form distinct peaks centered around 50 eV and 40 eV, respectively. Included for He are the results of calculations performed within various approximations. Of these, the first order Born approximation (FBA) and distorted-wave approach (DWA) of Mandal et al. [16] both predict a shape similar to experi-

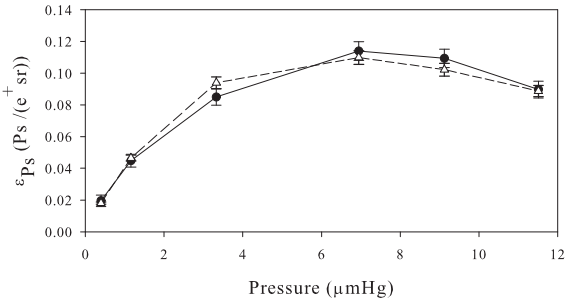

FIG. 1. The Ps beam production efficiency (bullet) of CO_2 at a Ps energy of 20 eV. The corresponding prediction (triangle) using the weighted mean of $\frac{dQ_{Ps}}{d\Omega}$ (from the data in Figure 2) is also shown.

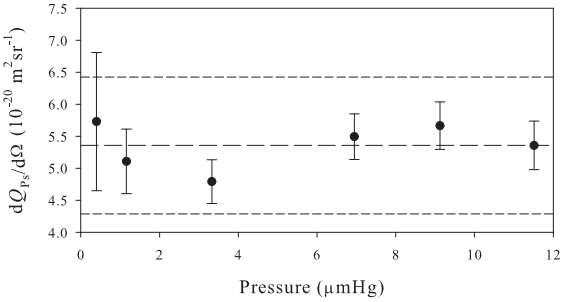

FIG. 2. Example of the absolute differential cross-section for Ps formation near zero degrees obtained using Equation 5: the target is CO_2 and the positron incident energy is 27 eV. Mean (long dash); ±3 standard deviations from the mean (short dash).

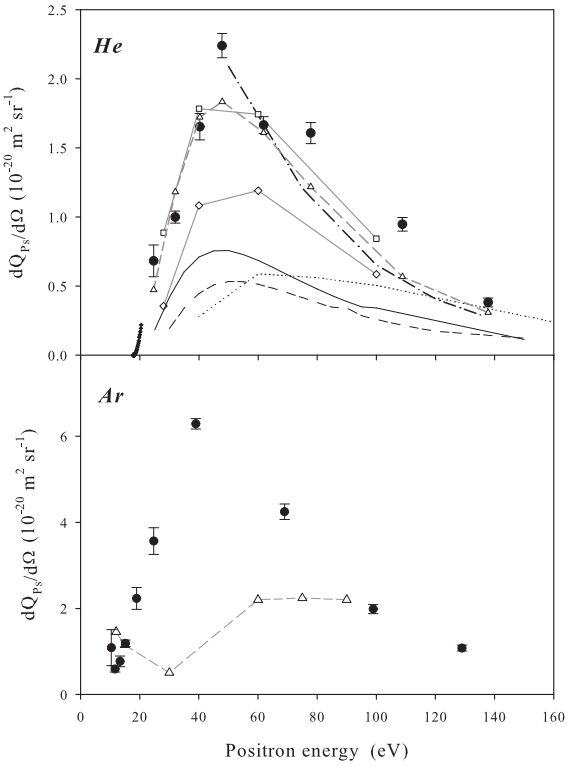

FIG. 3. The experimental absolute differential Ps(n=1) formation cross-section for positron scattering from atoms compared with theoretical results: (bullet) this work. He: (diamond) FBA [16]; (square) DWA [16]; (dotted line) close-coupling [19]; (dash dot) eikonal approximation [21]; (double dash) DWA [25]; (solid line) second order DWA [26]; (triangle) 27-state coupled-pseudostate approach [29, 58]; (thick line near the threshold), Kohn variational method [59]. Ar: (triangle) truncated coupled-static [24].

ment; the DWA also agrees in magnitude. However other DWA results [25, 26], although also similar in shape, are considerably lower especially in the peak region. The main differences between the various DWA calculations is in the form of the target wavefunction used and the fact that exchange was not included explicitly in work of Mandal et al. [16] who multiplied both the differential and integrated cross-sections obtained by a factor of two. The results of an eikonal approximation [21] have a magnitude close to experiment at the lowest energy considered but which decreases at a somewhat faster rate. The close-coupling calculations for positron-helium scattering are expected to give more accurate results than the methods discussed above as they include a better representation of the target and Ps distortions. The calculations of Chaudhuri and Adhikari [19] which include 5 states of He and 3 of Ps reveal a much broader maximum than seen experimentally and its magnitude is approximately a factor of 4 lower around the peak. A good agreement is found with the more elaborate 27-state coupled-pseudostate approximation of Walters and co-workers [29, 58] which include 3 Ps eigenstates, 6 He eigenstates and 18 He pseudostates. At low energies, the theoretical results display the same rapid rise as experiment and, although they are lower in magnitude at the peak itself, they agree with its the position. In the intermediate region, this theory is approximately (20-30)% below experiment, merging with it at the highest energy considered. The variational results in the Ore gap [59] display a very rapid rise from threshold. The calculations are based on the Kohn variational method for partial waves l=0 to 4 and the Born approximation for $5 \leq l \leq 10$; the uncertainty due to the use of the Born approximation is estimated to be at most (5 - 10)% [59]. It is worth noting that, over the energy range considered, the differential cross-sections predicted by [29, 59] have been found to change by less than 2% over the angular acceptance of the experiment, supporting the assumption made in Equation (3).

In the case of Ar, the experimental results are compared with the only available theory, a truncated static-coupled approximation [24]. This shows an initial decrease from 10 eV to 30 eV, increasing again at 60 eV, being close to experimental values at 10 eV and 90 eV.

Differential cross-sections for Ps formation from H_2

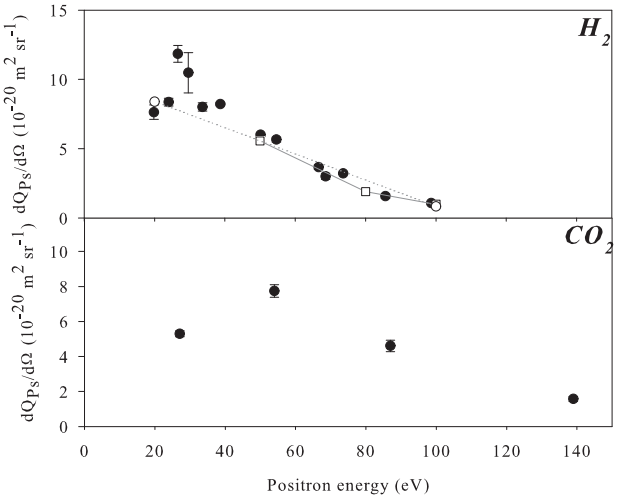

FIG. 4. Experimental absolute differential cross-sections for Ps formation from H_2 and CO_2 (bullet). Two theories are also shown for H_2: (hollow circle) FBA [18]; (square) second-order Born approximation [17].

and CO_2 are shown in Figure 4. In the case of H_2, the experimental data indicate a peak around 30 eV and are broadly consistent with the predictions of both first- and second-order Born determinations [17, 18]. In the case of CO_2, the differential cross-section displays a broad peak between 30 to 90 eV before decreasing at 140 eV.

In order to discern the degree of forward collimation of the Ps formed from each target, the energy dependence of the ratio $\frac{dQ_{Ps}}{d\Omega}/Q_{Ps}$ for He and Ar, and H_2 and CO_2 is plotted in Figure 5 a) and b) respectively. Experimental values have been calculated using the present measurements for $\frac{dQ_{Ps}}{d\Omega}$ and Q_{Ps}(all n) from various experiments [57, 60–62]. For He and Ar, this ratio is found to increase with energy, that for He being higher than for Ar. The ratio for H_2 is roughly twice as high as for CO_2. The greater yield of forward collimation for the low-Z targets (He and H_2) may be due to a comparatively weaker (repulsive) static interaction (e.g. [63]) and/or the influence of the angular momenta of the captured electrons (e.g. [64]).

Also shown in Figure 5 are theoretical values for He. Where possible, Q_{Ps} have been sourced from the same papers as the $\frac{dQ_{Ps}}{d\Omega}$ shown in Figure 3, or from other work which relies on the same approach (as in the case for the close-coupling approximation [19, 65]). However, in all cases except for the results of [59] and [29], the theoretical ratios should be considered overestimates (by around 20% or so) since their Q_{Ps} refer to n=1 or n=1,2 only. Even so, bar for those of Mandal et al. [16], these ratios are lower than experiment. Once again, a good agreement is found between experiment and the coupled-pseudostate calculation of [29] for $\frac{dQ_{Ps}}{d\Omega}$(n=1)/Q_{Ps}(all n) who allowed for n=1,2 formation explicitly and n>2

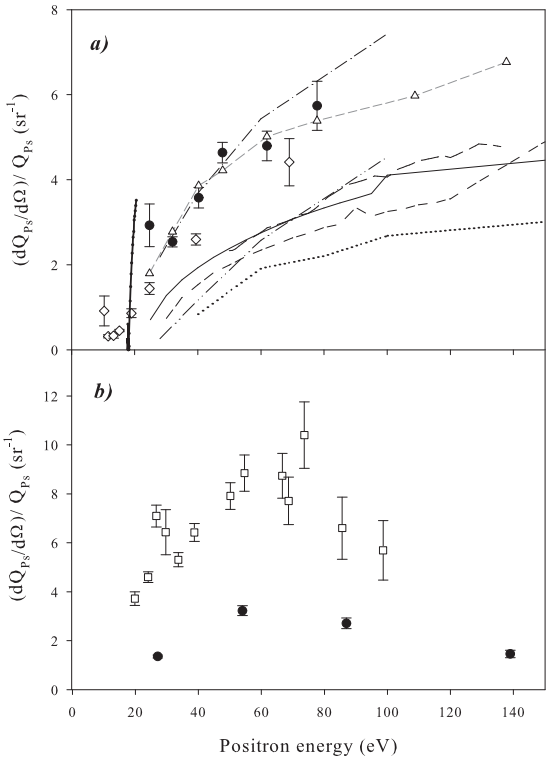

FIG. 5. A comparison of the ratio $\frac{dQ_{Ps}}{d\Omega}/Q_{Ps}$ for the atoms and molecules investigated in this work. a): (bullet) He; (diamond) Ar. Also shown in a) are $\frac{dQ_{Ps}}{d\Omega}/Q_{Ps}$ for the He theories shown in Figure 3: (dash double dot) FBA [16]; (dash dot) DWA [16]; (dotted line) close-coupling [19, 65]; (double dash) DWA [25]; (solid line) second order DWA [26]; (dash) eikonal approximation [21]; (triangle) 27-state coupled-pseudostate [29, 58]; (thick line near the threshold), Kohn variational method [59]. b): (square) H_2; (bullet) CO_2.

through the $1/n^3$ scaling [58]. The Kohn variational theory of [59], which is limited to energies below the Ps(n=2) threshold, indicates a very sharp rise up to a value of ~ 3.5 at 2.6 eV above it; that for the coupled-pseudostate results of [29] appears much more gradual.

In conclusion, the first measurements of the absolute differential Ps formation cross-sections have been presented for He, Ar, H_2 and CO_2. This work provides the only experimental test of a considerable body of theoretical work developed on the subject over the past 40 years [8–34, 58, 59]. In the case of He, the present measurements are in good agreement with the close-coupling results of [29, 58] and are not inconsistent with the near-threshold Kohn variational theory of [59]. Future lower energy measurements should enable a more stringent discrimination between the two theoretical descriptions. The results for H_2 are broadly consistent with the predictions of both the first- and second-order Born approximations in [17, 18]. We have found that the general shape of the cross-sections is similar for all four targets. It is

expected that the great sensitivity of theoretical angular-resolved cross-sections to the details of the various approximations (as illustrated in Figures 3 and 5) will also significantly impact on the resolution of the persistent discrepancies for the *integral* Ps formation cross-section (e.g. [3]).

The Engineering and Physical Sciences Research Council is gratefully acknowledged for supporting this work under grant no. EP/J003980/1 and for providing M.S. and S.E.F. with research studentships. The authors would like to thank James Walters and John Humberston for invaluable discussions and, together with Chandana Sinha, for making available tabulated data prior to publication.

[1] J. C. Higdon, R. E. Lingenfelter, and R. E. Rothschild, Astrophys. J. **698**, 350 (2009).
[2] W. Lehnert, M.-C. Gregoire, A. Reilhac, and S. R. Meikle, Phys. Med. Biol **56**, 3313 (2011).
[3] G. Laricchia, S. Armitage, A. Kövér, and D. J. Murtagh, Adv. At., Mol., Opt. Phys. **56**, 1 (2008).
[4] G. Laricchia, D. A. Cooke, A. Kövér, and S. J. Brawley, *Fragmentation Processes Topics in Atomic and Molecular Physics*, edited by C. T. Whelan (Cambridge University Press, 2013) p. 116.
[5] D. J. Murtagh, C. Arcidiacono, Z. D. Pesic, and G. Laricchia, Nucl. Instrum. Methods Phys. Res., Sect. B **247**, 92 (2006).
[6] D. J. Murtagh, D. A. Cooke, and G. Laricchia, Phys. Rev. Lett. **102**, 133202 (2009).
[7] D. A. Cooke, D. J. Murtagh, and G. Laricchia, Phys. Rev. Lett. **104**, 073201 (2010).
[8] N. Yamanaka and Y. Kino, Phys. Rev. A: At., Mol., Opt. Phys. **64**, 042715 (2001).
[9] B. H. Bransden and C. J. Noble, J. Phys. B: At., Mol. Opt. Phys. **32**, 1305 (1999).
[10] S. Kar and P. Mandal, Phys. Rev. A: At., Mol., Opt. Phys. **59**, 1913 (1999).
[11] S. Tripathi, C. Sinha, and N. C. Sil, Phys. Rev. A: At., Mol., Opt. Phys. **39**, 2924 (1989).
[12] A. Igarashi and N. Toshima, Phys. Rev. A: At., Mol., Opt. Phys. **46**, R1159 (1992).
[13] R. J. Drachman and K. Omidvar, Phys. Rev. A: At., Mol., Opt. Phys. **14**, 100 (1976).
[14] M. Z. M. Kamali and K. Ratnavelu, Phys. Rev. A: At., Mol., Opt. Phys. **65**, 014702 (2001).
[15] S. Kar and P. Mandal, Phys. Rev. A: At., Mol., Opt. Phys. **62**, 052514 (2000).
[16] P. Mandal, S. Guha, and N. C. Sil, J. Phys. B: At., Mol. Opt. Phys. **12**, 2913 (1979).
[17] P. K. Biswas and A. S. Ghosh, J. Phys. B: At., Mol. Opt. Phys. **30**, 983 (1997).
[18] P. K. Biswas, T. Mukherjee, and A. S. Ghosh, J. Phys. B: At., Mol. Opt. Phys. **24**, 2601 (1991).
[19] P. Chaudhuri and S. K. Adhikari, Phys. Rev. A: At., Mol., Opt. Phys. **57**, 984 (1998).
[20] N. K. Sarkar, M. Basu, and A. S. Ghosh, Phys. Rev. A: At., Mol., Opt. Phys. **45**, 6887 (1992).
[21] B. Nath and C. Sinha, Eur. Phys. J. D **6**, 295 (1999), and private communication.
[22] P. Chaudhuri, S. Adhikari, B. Talukdar, and S. Bhattacharyya, Eur. Phys. J. D **5**, 217 (1999).
[23] D. R. Schultz, C. O. Reinhold, and R. E. Olson, Phys. Rev. A: At., Mol., Opt. Phys. **40**, 4947 (1989).
[24] M. T. McAlinden and H. R. J. Walters, Hyperfine Interact. **89**, 407 (1994).
[25] S. Sen and P. Mandal, Phys. Rev. A: At., Mol., Opt. Phys. **80**, 062714 (2009).
[26] S. Sen, P. Mandal, and P. K. Mukherjee, Eur. Phys. J. D **66**, 230 (2012).
[27] E. Ghanbari-Adivi and A. N. Velayati, J. Phys. B: At., Mol. Opt. Phys. **46**, 065204 (2013).
[28] E. Ghanbari-Adivi, Braz. J. Phys. **42**, 172 (2012).
[29] H. R. J. Walters, in preparation and private communication (2015).
[30] F. A. Gianturco and R. Melissa, Phys. Rev. A: At., Mol., Opt. Phys. **54**, 357 (1996).
[31] S. Tripathi and C. Sinha, Phys. Rev. A: At., Mol., Opt. Phys. **42**, 5743 (1990).
[32] S. N. Nahar and J. M. Wadehra, Phys. Rev. A: At., Mol., Opt. Phys. **35**, 4533 (1987).
[33] P. S. Mazumdar and A. S. Ghosh, Phys. Rev. A: At., Mol., Opt. Phys. **34**, 4433 (1986).
[34] O. A. Fójon, R. D. Rivarola, J. Hanssen, and P. A. Hervieux, J. Phys. B: At., Mol. Opt. Phys. **34**, 4279 (2001).
[35] S. Tang and C. M. Surko, Phys. Rev. A: At., Mol., Opt. Phys. **47**, R743 (1993).
[36] T. Falke, T. Brandt, O. Kuhl, W. Raith, and M. Weber, J. Phys. B: At., Mol. Opt. Phys. **30**, 3249 (1997).
[37] R. M. Finch, A. Kövér, M. Charlton, and G. Laricchia, J. Phys. B: At., Mol. Opt. Phys. **29**, L667 (1996).
[38] S. Armitage, D. E. Leslie, A. J. Garner, and G. Laricchia, Phys. Rev. Lett. **89**, 173402 (2002).
[39] D. E. Leslie, S. Armitage, and G. Laricchia, J. Phys. B: At., Mol. Opt. Phys. **35**, 4819 (2002).
[40] M. Shipman, S. Brawley, D. Leslie, S. Armitage, and G. Laricchia, Eur. Phys. J. D **66**, 96 (2012).
[41] G. Laricchia and H. R. J. Walters, Riv. Nuovo Cimento **35**, 305 (2012).
[42] A. J. Garner, A. Özen, and G. Laricchia, Nucl. Instrum. Methods Phys. Res., Sect. B **143**, 155 (1998).
[43] G. Laricchia, S. Armitage, and D. E. Leslie, Nucl. Instrum. Methods Phys. Res., Sect. B **221**, 60 (2004).
[44] A. J. Garner, G. Laricchia, and A. Özen, J. Phys. B: At., Mol. Opt. Phys. **29**, 5961 (1996).
[45] M. Shipman, S. J. Brawley, L. Sarkadi, and G. Laricchia, Eur. Phys. J. D **68**, 66 (2014).
[46] K. R. Hoffman, M. S. Dababneh, Y. F. Hsieh, W. E. Kauppila, V. Pol, J. H. Smart, and T. S. Stein, Phys. Rev. A: At., Mol., Opt. Phys. **25**, 1393 (1982).
[47] W. E. Kauppilla, T. S. Stein, J. H. Smart, M. S. Dababneh, Y. K. Ho, J. P. Downing, and V. Pol, Phys. Rev. A: At., Mol., Opt. Phys. **24**, 725 (1981).
[48] C. K. Kwan, Y.-F. Hsieh, W. E. Kauppila, S. J. Smith, T. S. Stein, M. N. Uddin, and M. S. Dababneh, Phys. Rev. A: At., Mol., Opt. Phys. **27**, 1328 (1983).
[49] P. Caradonna, A. Jones, C. Makochekanwa, D. S. Slaughter, J. P. Sullivan, and S. J. Buckman, Phys. Rev. A: At., Mol., Opt. Phys. **80**, 032710 (2009).
[50] S. J. Brawley, S. Armitage, J. E. Beale, D. E. Leslie, A. I.

Williams, and G. Laricchia, Science **330**, 789 (2010).
[51] A. J. Garner, A. Özen, and G. Laricchia, J. Phys. B: At., Mol. Opt. Phys. **33**, 1149 (2000).
[52] S. J. Brawley, A. I. Williams, M. Shipman, and G. Laricchia, Phys. Rev. Lett. **105**, 263401 (2010).
[53] W. E. Kauppila and T. S. Stein, *Advances in Atomic, Molecular and Optical Physics*, edited by D. Bates and B. Bederson, Vol. 26 (Academic Press, San Diego, 1990).
[54] M. S. Dababneh, W. E. Kauppila, J. P. Downing, F. Laperriere, V. Pol, J. H. Smart, and T. S. Stein, Phys. Rev. A: At., Mol., Opt. Phys. **22**, 1872 (1980).
[55] A. Zecca, L. Chiari, A. Sarkar, K. L. Nixon, and M. J. Brunger, Phys. Rev. A: At., Mol., Opt. Phys. **80**, 032702 (2009).
[56] A. Zecca, L. Chiari, E. Trainotti, D. V. Fursa, I. Bray, A. Sarkar, S. Chattopadhyay, K. Ratnavelu, and M. J. Brunger, J. Phys. B: At., Mol. Opt. Phys. **45**, 015203 (2012).
[57] S. Zhou, H. Li, W. E. Kauppila, C. K. Kwan, and T. S. Stein, Phys. Rev. A: At., Mol., Opt. Phys. **55**, 361 (1997).
[58] C. P. Campbell, M. T. McAlinden, A. A. Kernoghan, and H. R. J. Walters, Nucl. Instr. Meth. B **143**, 41 (1998).
[59] P. Van Reeth and J. W. Humberston, J. Phys. B: At., Mol. Opt. Phys. **32**, 3651 (1999) and in preparation (2015).
[60] D. J. Murtagh, M. Szłuińska, J. Moxom, P. Van Reeth, and G. Laricchia, J. Phys. B: At., Mol. Opt. Phys. **38**, 3857 (2005).
[61] G. Laricchia, P. Van Reeth, M. Szłuińska, and J. Moxom, J. Phys. B: At., Mol. Opt. Phys. **35**, 2525 (2002).
[62] D. A. Cooke, D. J. Murtagh, and G. Laricchia, J. Phys. Conf. Ser. **199**, 012006 (2010).
[63] G. Laricchia, Nucl. Instrum. Methods Phys. Res., Sect. B **99**, 363 (1995).
[64] J. Moxom, G. Laricchia, M. Charlton, A. Kövér, and W. E. Meyerhof, Phys Rev A **50**, 3129 (1994).
[65] S. K. Adhikari and A. S. Ghosh, Chem. Phys. Lett. **262**, 460 (1996).